MRI texture analysis in the abdomen and pelvis

Thomas JV, Abou Elkassem A, Ganeshan B, Smith AD

Version 11 (final)

KEY WORDS

- MR Imaging
- Texture Analysis
- Liver Pathology
- Prostate Cancer
- Rectal Carcinoma
- Renal Cell carcinoma
- Pancreatic Carcinoma
- Endometrial Carcinoma
- Non-Hodgkin Lymphoma
- Crohn's Disease

KEY POINTS

- Texture analysis is a form of radiomics and refers to quantitative measurements of the histogram, distribution and/or relationship of pixel intensities or gray scales within a region of interest on an image.
- MRI texture analysis minimizes variability related to subjective reader interpretation of image heterogeneity.
- MRI texture analysis is highly impacted by image acquisition and reconstruction parameters. However, use of maps as against weighted MRI images and few selected global texture parameters post filtration (having biological correlates) rather than using multiple (redundant and less-reproducible), local-regional parameters has shown better repeatability in some studies.
- MRI texture analysis has multiple clinically - relevant potential applications in the abdomen and pelvis, including tissue characterization and cancer response evaluation or prediction of outcomes in various tumors.

Synopsis

Texture analysis (TA) is a form of radiomics and refers to quantitative measurements of the histogram, distribution and/or relationship of pixel intensities or gray scales within a region of interest on an image. TA can be applied to MRI of the abdomen and pelvis, with the main strength being quantitative analysis of pixel intensities and heterogeneity rather than subjective/qualitative analysis. There are multiple limitations of MR texture analysis (MRTA) including a dependency on image acquisition and reconstruction parameters, non-standardized approaches without or with image filtration, diverse software methods and applications, and statistical challenges relating numerous texture analysis results to clinical outcomes in retrospective pilot studies with small sample sizes. Despite these limitations, there is a growing body of literature supporting MRTA. In this review, the application of MRTA to the abdomen and pelvis will be discussed, including tissue or tumor characterization and response evaluation or prediction of outcomes in various tumors.

Fundamentals of Texture Analysis

Texture analysis (TA) refers to quantitative measurements of the histogram, distribution and/or relationship of pixel intensities or gray scales within a region of interest (ROI) on an image (1,2). In the abdomen and pelvis, TA is commonly performed on CT and MRI. This review will focus on the application of MRI TA as part of the evolving field of radiomics, defined by high-throughput extraction of quantitative imaging features and the associated analysis and interpretation as it relates to a physiologic or pathologic process. TA is often performed on 2D

ROIs, which is enough for many applications, but volumetric or 3D TA is also possible, particularly for large structures (e.g. the liver) or a locoregional disease (1,2).

There are different methods of TA including statistical-, model-, and transform-based methods (1,2). The most utilized form of TA is first-order statistics which evaluates the distribution (frequency of occurrence not the spatial relationship) of gray-levels in a pixel-intensity histogram (**Fig.1**). Commonly used first-order statistics including mean, standard deviation(SD), threshold, minimum, maximum, skewness, kurtosis, and entropy (**Fig. 2**). Second-order statistics analyze texture in a specific direction and length and can be derived from a run-length matrix or a co-occurrence matrix. Higher-order statistics evaluate location and relationships between three or more pixels and can be derived from neighborhood gray-tone difference matrices. MRTA involves multiple steps from image acquisition through classification (**Fig. 3**).

Many texture parameters are sensitive to multi-parametric(mp)-MR acquisition and reconstruction parameters (1-5) whereby sequence-type, flip-angle, TR, TE, FOV, contrast, slice-thickness, and reconstruction-algorithms affect pixel intensities, spatial relationships, and edges. In order to minimize these effects, standardization of image protocols and the use of image filtration methods have been utilized (1,2). MRI maps are more quantitative than weighted images. Amongst the maps - Dixon (fat and water) maps are one of the most robust and reproducible MR sequence followed by ADC maps and T1/T2 maps.

The purpose of image filtration prior to performing TA is to reduce the effect of technical aspects on measurement of TA parameters (1,2). Commonly used filtration methods include Laplacian of Gaussian filter, though many other filtration methods are possible. The filters are

intended to standardize the image pixel signal intensity patterns across a range of image acquisition and reconstruction parameters and allow for extraction of specific features corresponding to the width of the filter imperceptible to the naked eye. Fine, medium and coarse texture features are emphasized with lower to higher filter values. Pre-processing methods for standardizing image filtration, segmentation, edge erosion, and image processing are lacking.

TA requires an advanced image processing tool, and these tools are becoming more common and incorporated into commercial platforms(1,2)e.g.TexRAD (https://fbkmed.com/texrad-landing/). However, there is little standardization in approach between different systems, making it challenging to reproduce and validate study results. A standardized approach is needed(6), and open source methods such as PyRadiomics (https://pyradiomics.readthedocs.io/en/latest/) may provide such a solution.

Another major challenge with MRTA is the volume of data that is produced, with many texture tools generating hundreds or thousands of measurements. Not only is it difficult or impossible to understand the meaning of all the texture parameters, but it is also statistically challenging to identify true relationships between one or more texture parameters and a biologic outcome (1,2). Machine learning algorithms are often able to find relationships between a multitude of measurements and an outcome; though in a non-intuitive manner and the problem of a type I error still exists, particularly when the number of measurements exceeds the patient sample size (1,2). To address this, a simulation and phantom study by Miles et al. (7) demonstrated what filtration-histogram based TA actually means and how it is associated with different components of heterogeneity like object size, density of objects in

relation to the background and number/concentration of objects. Gourtsoyianni et al. (8, 9) in their MRTA demonstrated that repeatability is better for global texture parameters post-filtration than for local-regional texture parameters.

The ideal TA parameter is both accurate (strongly associated with a meaningful outcome) and precise (repeatable across different acquisition parameters and time, reproducible across different MRI scanners, and associated with high intra- and inter-observer agreement) (1,2). Despite multiple limitations, MRTA has had a major impact on abdominal imaging research. The remainder of this article will review the impact of MRTA on liver pathology, prostate, rectal, renal cancers and other abdominal pathologies.

MRTA for Liver Pathology

A great use case for MRTA is to stage hepatic fibrosis **(Fig. 4)** as MRI is noninvasive and the liver is a large organ. Studies have shown that MRTA can be successfully used to differentiate cirrhotic patients from healthy volunteers (10). TA can be performed on a variety of MRI sequences including T1-weighted, T2-weighted, Proton density (PD), Diffusion weighted Images (DWI) and Post contrast enhanced images (11-14).

Studies on murine models (15) using T1-maps have shown excellent discrimination of hepatic fibrosis within histogram and Gray Level Gradient Matrix (GLGM) categories. Histogram Inter quartile range (IQR) achieved an AUC of 0.90 ($p<0.0001$) and GLGM feature variance gradient achieved an AUC of 0.91 ($p< .0001$). In human subjects, Canella et al (16) using first order statistical approach extracted TA parameters on non-contrast 3D-GRE T1-weighted images in 54 patients with Non-alcoholic Fatty Liver Disease (NAFLD). SD and entropy demonstrated moderate statistically significant correlation ($p<0.01$) with degree of significant

and advanced hepatic fibrosis in patients with NAFLD. However, the correlation between TA parameters and other histopathological features were weak and not statistically significant in this study.

Yu et al. (15) demonstrated good to excellent discrimination of hepatic fibrosis on T2 maps in murine models within histogram, Gray Level Co-occurrence Matrix (GLCM), Gray Level Run Length (GLRL) and GLGM categories. GLGM feature kurtosis was the best discriminator of hepatic fibrosis, achieving an AUC value of 0.90 ($p<0.0001$). House et al (17) showed an AUC of 0.51-0.74 for advanced fibrosis using 14 Harlick TA parameters extracted on T2-weighted images in 49 patients with NAFLD. Wu et al. (18) applied TA on T2-weighted, pre and post contrast T1-weighted images (n=279 parameters) in 125 patients with chronic hepatitis C and reported misclassification rates for fibrosis stage and necro-inflammatory activity grade as high as 35.77% and 34.15% respectively. Eng et al. (10) studied 43 patients divided into four groups according to their clinical stage and 10 controls using a T2-weighted breath-hold sequence on a 1.5 T scanner. First- and second-order TA parameters and several classification methods were applied to differentiate patients and controls. All the statistical methods were able to differentiate between controls and patients in each group. The classification error varied around 8%.

Yu et al. (19) also analyzed the role of MRI PD images, quantifying hepatic fibrosis in murine models. Histogram features demonstrated very weak to moderate correlations (r=-0.29-0.51) with hepatic fibrosis. GLCM features correlation and contrast demonstrated moderate to strong correlations (r=-0.71 and 0.59) respectively with hepatic fibrosis. Moderate correlations were seen between hepatic fibrosis and the GLRL feature short run low gray level emphasis (SRLGE)

(r=-0.51). GLGM features demonstrated weak to very weak correlations with hepatic fibrosis (r=-0.27 to 0.09). Moderate correlations were seen between hepatic fibrosis and Law's features, L6 and L7 (r=0.58). To our knowledge, no studies using MRI PD for TA has been performed in human subjects.

Barry et al. (20) evaluated the application of TA to DWI in murine models. The median hepatic ADC values, correlation feature values (GLCM) and GLRL features achieved the highest correlation with digital image analysis derived assessment of fibrosis, with a very strong correlation of (r=-0.89), (r=0.69) and (r=-0.86) respectively.

Hepatic fibrosis evaluated in rats by Xu et al. (21) demonstrated that only a few texture features at certain filter setting of post-enhanced T1 mapping images and T1 mapping showed statistical differences. Kato et al. (22) evaluated liver parenchymal textures on MR images of 52 patients who underwent partial hepatectomy and demonstrated that the accuracy was greater for Gadolinium enhanced equilibrium phase images (AUC=0.801) than for T1-weighted images (AUC=0.597) or T2-weighted images (AUC=0.525, $p<0.05$), and the outputs of equilibrium phase images showed moderate correlation (r=0.502, p=0.001) with the pathologic grades. The radiologist interpretations of all images combined (AUC=0.503, $p<0.05$), and the confidence of all images were moderately correlated (r=0.473, p=0.002) with pathological grades. However, the accuracy of equilibrium phase images in the computer algorithm (AUC=0.801) was greater that the equilibrium phase images of the radiologists (AUC=0.546). Bahl et al. (13) demonstrated cross-validated sensitivity of 91.9%, specificity of 83.9% and total accuracy of 88.2% in contrast enhanced models of 68 patients with diffuse liver disease with histology-based staging of fibrosis.

TA can be applied either prospectively or retrospectively on routine cross-sectional imaging, without the need for dedicated hardware. Results of TA however depends on image quality and the placement of ROIs (15). 3T is better than 1.5T in classifying liver fibrosis and MR images have an advantage over CT images with regards to accuracy of texture features (23). The biggest limitation of TA for fibrosis is lack of standardization. Comparison between sites is challenging as different MRI sequences and TA features and combination of features have been reported in the literature. Within these constraints, the performance of TA of hepatic fibrosis AUCs varied from as low as 0.40 for detection of fibrosis stage > 3 and as high as 1.00 for staging of cirrhosis (15). This variability makes it difficult comparing different studies. Further standardization, larger studies and studies comparing texture analysis with other techniques for assessment of hepatic fibrosis are needed.

Hepatic hemangiomas (HH), hepatic metastasis (HM), hepatocellular carcinoma (HCC) are the common liver lesions that have an overlap of imaging findings on MRI (24). Li et al. analyzed the usefulness of Fat-saturated T2-weighted sequences in 162 patients on a 3T MR system in classification of these 3 lesions and demonstrated potential role of textural parameters in accurate detection and diagnosis of these lesions (25). Hepatic Adenoma (HA) and Focal Nodule Hyperplasia (FNH) are benign liver tumors commonly seen in young women (26). Differentiating HA from FNH has clinical significance. Gadoxetic acid enhanced MRI is widely used for differentiation of HA from FNH. A recent meta-analysis (27) showed lesion hypointensity on the hepatobiliary phase (HBP) had a pooled sensitivity of 95% and specificity of 92% for differentiating HA from FNH. However, 7-26% of HAs are iso- to hyperintense, and 3-8% of FNHs are hypointense to background hepatic parenchyma on the HBP (28). Canella et al. (28)

demonstrated that TA may have an added value for diagnosis of atypical HA that present without hypointensity on the HBP imaging with Gadoxetic acid. A skewness value on HBP of greater than –0.06 had a sensitivity of 72.5% and a specificity of 90.6% for diagnosis of HA in this study.

When attempting to differentiate benign hepatic tumors (FNH, HA) from HCC, Stocker et al. (29) reviewed MRI scans from 108 non-cirrhotic patients from a multi-center study. These scans were performed at different centers on 1.5T scanners using a variety of Gadolinium based contrast agents. Despite a significant overlap in imaging findings, the most promising results was for the TA of arterial phase images able to distinguish HCC from benign liver lesions with a sensitivity of 84.9% and a specificity of 84.1%, outperforming the conventional readings of images in the study.

HCC, one of the leading cause of cancer deaths worldwide requires accurate staging for optimizing treatment and prognosis. Low grade HCC mostly have high survival rates whereas high grade tumors are at high risk and often require special treatment (30,31). Zhou et al. evaluated 46 patients with resected HCC who underwent contrast enhanced MRI (32). **(Fig. 5)** Low grade HCCs were found to have higher average signal intensity values and decreased GLN on the arterial phase, compared to high grade HCCs (p=0.0005) and showed potential applications in predicting the histological grade of HCC preoperatively.

Hepatic resection is the primary treatment option for HCC with well- preserved hepatic function (33). Recurrence can be as high as 50% within 5 years (34) and intra-hepatic distant recurrence tends to have the worst prognosis (35). Given limited organ availability and the invasive nature of surgical intervention, identifying patients with long-term curative outcome

without recurrence is important. Ahn et al. (36) analyzed preoperative MRI findings in 179 patients with a single HCC and found that satellite nodules, peritumoral hypointensity, absence of capsule and lower GLCM angular second moment (ASM) were predictors for early recurrence ($p < 0.05$). Hui TCH et al (37), demonstrated in a retrospective study of 50 patents that single variables from TA of contrast enhanced MRI images may be able to predict early HCC recurrence with high accuracy (78-84% equivalent to AUC=0.78-0.84).

Trans-arterial chemoembolization (TACE), Trans-arterial radioembolization (TARE) and high frequency ultrasound (HIFU) are minimally invasive/ non-invasive methods of tumor treatment. Yu et al. (38) evaluated 89 subjects with HCC that had TA based contrast enhanced MRI before and 1 week after TACE/ HIFU and demonstrated that patients who had complete response (n=58) showed higher uniformity and energy but lower entropy and skewness than the non-complete response group (n=31) ($p<0.05$). The study showed that logistic regression and ROC analysis of entropy before TACE/HIFU and skewness and entropy 1 week after treatment were predictors of an early response. TARE evaluated by Reimer et al. (39) in 37 patients demonstrated that MRI based TA showed an earlier differentiation between patients with and without progressive disease. Chemotherapeutic response of colorectal liver metastasis in 26 patients were retrospectively evaluated by Zhang et al. (40) and showed that MRTA on pre-treated T2 images have the potential to predict the therapeutic response of colorectal liver metastasis.

MRTA for Prostate Carcinoma

mpMRI has revolutionized the detection, staging and management of early prostate carcinoma. mpMRI consists of T2, T1 weighted images, diffusion-weighted images (DWI) and

contrast enhanced T1 weighted perfusion images (41). Wibmer et al. analysis of 147 patients demonstrated that several Haralick texture features derived from T2 and ADC maps have the potential to differentiate non-cancerous from cancerous prostate tissue. They also demonstrated that tumor energy and entropy on ADC maps in the peripheral zone (PZ) correlate with Gleason score and that T2- weighted image derived TA features are not associated with Gleason score (42). **(Fig. 6)**

The histological Gleason score (GS) is essential for the management of prostate carcinoma. The D'Amico risk stratification score, which is frequently used, uses a combination of clinical and imaging data with histology to gauge the 5-year risk of treatment failure. Current risk stratification uses clinical examination, serum Prostate Specific Antigen (PSA) and transrectal prostate biopsy. Hameed et al. (43) however demonstrated that when using ADC map mpMRI TA, there was a negative correlation with Gleason score. Post-contrast TA features also negatively correlated with the D'Amico score. When evaluating the TA of single sequences, Nkethiah et al. (44) demonstrated that T2 weighted MRI derived TA correlate significantly with Gleason score. In addition, the ADC TA were able to differentiate Gleason score 3+4 from 4+3 cancers and also augment tumor characterization. Rozenberg et al. (45) on the other hand demonstrated that whole lesion mean ADC, ADC ratio and ADC histogram analysis were not predictive of pathologic upgrading of GS 3+4=7 after radical prostatectomy and were not able to differentiate Gleason score 3+4 from 4+3 grade tumors. ADC TA however did improve accuracy.

Transition zone (TZ) tumors remain more difficult to appreciate on mpMRI images (46); with reported sensitivity/ specificity of 0.53/0.83 compared with 0.80/0.97 for PZ. Sidhu et al. (47)

demonstrated that MRTA features can discriminate significant prostate carcinoma of TZ. Significant tumor demonstrated a less peaked ADC histogram and revealed higher post-contrast T1-weighted homogeneity.

Like mpMRI, mpMRTA of multiple sequences has shown to lead to better classification results than a single sequence (48,49). However, recent studies (50,51) have shown the accuracy of bi-parametric MRI (T2-weighted imaging and DWI) for tumor detection is equal to that of traditional mpMRI. Niu et al. (52) in their retrospective study of 184 patients on a 1.5T scanner concluded that bi-parametric MRI-based TA may contribute to the detection and risk stratification of high-grade prostate carcinoma without the need for additional MRI sequences such as dynamic contrast enhanced (DCE) series.

External beam radiotherapy is standard treatment for localized prostate carcinoma. The 5-year biochemical recurrence rates are reported at 0-10%, 10-20% and 30-40% for the low, intermediate and high-risk groups respectively (53). These risk groups however are heterogeneous in terms of radiosensitivity, making it important to identify other predictors of recurrence. Gnep et al (54) retrospectively analyzed 74 patients with PZ localized prostate carcinoma on pre-radiotherapy 3T MRI. T2-Haralick features were found to be strongly associated with biochemical recurrence following radiotherapy.

Several nomograms, including the Kattan nomogram and Partin tables have been developed to predict the risk of prostate carcinoma progression after radical prostatectomy (RP) (55,56). However, only a few studies (55) showed an accuracy of 70% to predict PSA recurrence within 5 years of radical prostatectomy. Poulakis et al (57) tested the predictive ability of an Artificial Neural Network (ANN) for predicting biochemical recurrence, compared against Logistic

Regression Analysis (LRA), Han tables and the Kattan nomogram using AUC analysis of 191 consecutive patients, post RP and without nodal metastasis. The ANN was found to be superior to LRA and nomograms to predict biochemical recurrence accurately.

Bone metastasis occur in more than 90% of advanced prostate cancer (58). Standard imaging techniques such as technetium-99m bone scintigraphy and CT are incapable of assessing bone activity over time (59). Several studies have demonstrated the potential of DWI for monitoring treatment response of bone metastasis (60). Reischauer et al. (61) prospective analysis of data in 12 treatment naïve patients who had pre and post treatment 1.5T MRI indicated that whole-tumor volumetric TA may be utilized for response assessment in prostate cancer bone metastasis and could be used as a complementary measure for treatment monitoring in conjunction with averaged ADC values.

MRTA for Rectal Carcinoma

Rectal cancer, a subtype of colon cancer requires a dedicated multidisciplinary approach for management. Diagnostic imaging of the disease has significantly improved over the last few years through with MRI (62). Despite a prolonged learning curve, combined T2 morphology and qualitative/volumetric DWI evaluation form the cornerstone of clinically applicable daily rectal MRI interpretation (63). Multi-parametric MRI using conventional T2 weighted sequences has consistently demonstrated excellent accuracy in evaluating the relationship of the tumor with the meso-rectal fascia in treatment naïve patients (64). This is of prognostic importance because a positive circumferential resection margin (CRM) is an independent risk factor for local recurrence (65). However, determination of the T stage by conventional MRI remains challenging, with accuracy level before radiotherapy ranging from 66-88% (66).

Results of a number of MRI based studies have suggested that texture analysis may augment conventional imaging in cancer therapy response evaluation (67-69). Gourtsoyianni et al. (9) prospectively evaluated the repeatability of global and local MR texture features in 14 patients with rectal cancer. They found that MR imaging repeatability was better and robust for global texture parameters of the tumor than local regional texture parameters for clinical use.

An accurate imaging assessment of response to neoadjuvant therapy is crucial because of the differences in response based on tumor pathology (63). A large meta-analysis of MRI imaging showed a mean sensitivity of 50% and specificity of 91% to detect residual tumor using standard T2-weighted sequences during re-staging MRI post chemo-radiotherapy (CRT), with sensitivity improved after addition of DWI imaging, without affecting specificity (70). Yang et al. (71) retrospectively evaluated DWI in combination with TA in 76 patients with locally advanced rectal carcinoma (LARC) who underwent pre-operative CRT and subsequent surgery. Mean post CRT ADC values calculated for high-resolution DWI could select for patients with LARC who had a pathologic complete response (pCR). First order TA of T2-weighted images could also identify patients with pCR, even though they could not significantly improve diagnostic performance. De Cecco et al.(67) prospectively evaluated 15 consecutive patients with rectal carcinoma who underwent 3T imaging before and after neoadjuvant chemotherapy. TA parameters derived from T2-weighted images of rectal carcinoma, specifically kurtosis, demonstrated potential to act as imaging biomarkers of tumoral response to neoadjuvant chemotherapy. Pre-treatment kurtosis showed a sensitivity and specificity for pCR of 100% and 77.8% respectively. Aker et al. (72) retrospectively evaluated 114 patients with post-treatment MRI scans and were able to identify patients with complete response. AUC ranged from 0.750 to 0.88. Nardone V et al. (73)

retrospectively evaluated 49 rectal cancer patients treated with CRT and demonstrated that MRI TA could be used to identify patients with locally advanced rectal cancer with a higher risk of developing distant metastasis. GLCM was significantly higher in patients developing early disease progression. Jallil et al. (74) also showed that MRTA can act as an independent predictor of survival in patients with locally advanced rectal carcinoma.

MRTA for Renal Cell Carcinoma

Renal cell carcinomas (RCC) are classified into subtypes, most commonly clear cell, papillary and chromophobe (75). Subtyping RCCs affects treatment options and outcomes (76). The different RCC subtypes are known to have varying appearances on MRI, and TA has the potential to be used as a biomarker to classify RCC subtypes.

High stage clear cell RCC (ccRCC) is often heterogeneous in appearance on MRI due to co-occurrence of viable tumor and internal necrosis and hemorrhage. However, differentiating minimally aggressive from highly aggressive ccRCC can be challenging (77). Kierans et al. (78) retrospectively evaluated 61 patients with ccRCC who underwent pre-operative MRI at 1.5T. Their finding of lower ADC kurtosis in stage III and IV lesions likely reflects increased lesion heterogeneity secondary to increased cellularity, tumor necrosis and hemorrhage. High stage ccRCC were larger and had statistically significant higher ADC skewness and co-occurrence matrix correlation in their series.

Papillary RCC (pRCC) is the second most common subtype (75). Despite better prognosis of pRCC compared to ccRCC, several series have shown that the type 2 pRCC is associated with a higher nuclear grade and poorer survival than type 1 (78). Doshi et al. (80) retrospectively evaluated the qualitative and quantitative features in pre-operative MRI scans in patients with

pRCC, and multivariate logistic analysis showed that indistinct margins and heterogenous enhancement were independent predictors of papillary subtype (AUC=0.822). The quantitative univariate TA showed that the mean entropy was greater for the type 2 PRCC than in type 1 on ADC and contrast-enhanced nephrographic phase images (AUC=0.682-0.716). However, a combined qualitative and quantitative model were predictors of a subtype with good performance (AUC = 0.859). Vendrami et al. (81) in a similar study found that entropy was an independent predictor of type 2 tumors on all MRI sequences evaluated. In their series, combining the qualitative and quantitative features found that the probability calculated for the 2D TA of the VIBE sequence was a good predictor of type 2 tumors with good performance (AUC=0.87). Goyal et al. (82) retrospectively evaluated 33 patients with 34 RCC masses. Several MR texture parameters including enteropy, standard deviation, mean and skewness at different spatial scaling factors (SSF) for different MR sequences showed excellent diagnostic performance (AUC>0.8) in differentiating CC-RCC from NC-RCC and high grade from low grade CC-RCC.

MRTA for Other Abdominal and Pelvic Conditions

Quantitative MRI TA has also been attempted in a limited manner with other abdominal and pelvic organs. Pancreatic adenocarcinoma has a poor recurrence free and overall survival (83). Sensitivity and specificity of CT/MR in diagnosing tumor staging are approximately 60% and 90%, respectively (84). If pre-operative imaging can predict prognosis and the resectable status of the tumor, it would be extremely helpful. CTTA has been correlated with pathological results in a few studies (85,86) and shown to correlate with the outcomes of pancreatic adenocarcinoma patients. Choi et al. (87) have retrospectively evaluated 66 pancreatic

adenocarcinoma patients who had pre-operative 3T MRI scans and showed that tumor size was a significant predictive factor for both recurrence free and overall survival. However, other TA parameters which showed statistical significance to predict recurrence free and overall survival according to univariate analysis did not remain significant after multivariate analysis.

Endometrial cancer, is the most common female gynecological cancer (88). The PORTEC-1 trial (89) established certain factors for recurrence in early stage patients, further evaluated by the Gynecologic Oncology Group (GOG) study into a subgroup of patients considered "High Intermediate Risk" (HIR) group (90) based on age, tumor grade, lymphovascular space invasion and depth of myometrial invasion (91). MRI is an accurate imaging technique for the pre-operative assessment of endometrial cancer and for assessing depth of myometrial invasion (92,93). Dynamic contrast enhanced MRI (DCE-MRI) is considered more accurate than T2-weighted imaging in tumor detection and assessing depth of myometrial invasion (DMI) (94). Das et al. (95) in a systematic meta-analysis showed that DWI has a high sensitivity and specificity for detecting and ruling out DMI. Ueno et al. (96) retrospectively evaluated 137 patients with endometrial carcinoma measuring greater than 1 cm on a 1.5T system. TA was performed on T2-weighted, DWI, DCE images and ADC maps. The study demonstrated that MRTA with RF modeling allowed accurate diagnosis of the presence of depth of myometrial invasion, lymphovascular space invasion, and high tumor grade and achieved equivalent accuracy to that of subspecialty radiologists. Ytre-Hauge et al. (97) in a prospective study of 180 patients with endometrial cancer showed that MRI derived tumor texture parameters independently predicted DMI, high risk, histological subtype and reduced survival.

In patients with non-Hodgkin lymphoma (NHL), MRTA has been evaluated in a limited manner. Harrison et al. (98) evaluated MRI images of 10 NHL patients obtained on a 1.5T scanner, to see if TA parameters of MRI changed during chemotherapy. Patients were imaged in the diagnostic stage and four times after chemotherapy was started. The best discrimination was obtained within the T2-weighted images between the pre-treatment and the second imaging stage in all texture feature groups, suggesting it to be a promising quantitative means of demonstrating lymphoma tissue changes during chemotherapy.

MRTA has been evaluated in a limited manner in Crohn's disease. Makanyanga et al. (99) retrospectively evaluated 16 patients undergoing MR enterography before ileal resection. Their preliminary data suggested some MRTA parameters of T2-weighted images may be associated with histologic and MRI activity scores. Bhatnagar et al. (100) evaluation of seven Crohn's patients who underwent pre-ileal resection 3T MRI scans showed contrast enhanced MRTA features defer significantly between bowel exhibiting angiogenesis versus bowel that does not.

Summary

MRTA is a form of radiomics and refers to quantitative measurements of the distribution and relationship of pixel intensities within a region of interest. While TA minimizes variability related to subjective reader interpretation of image heterogeneity, MRTA is highly impacted by image acquisition and reconstruction parameters, making it difficult to reproduce and validate in external patient populations, thereby severely limiting adaptability to clinical practice. Use of maps as against weighted MRI images and use of global texture parameters such as filtration-histogram based technique reduces the variability and has shown to be reproducible. Also the

use of a few selected parameters having biological correlates is recommended rather than using multiple parameters which may be redundant and not reproducible.

Never-the-less, MRTA has multiple clinically-relevant potential applications in the abdomen and pelvis, including tissue characterization (e.g. staging of hepatic fibrosis, grading of prostate cancer, or subtyping of RCC) and cancer response evaluation or prediction of outcomes in various tumors (e.g. HCC, prostate cancer, RCC, rectal cancer, pancreatic adenocarcinoma, endometrial cancer, NHL, etc.). At present, most MRTA studies are pilot, exploratory, and retrospective in nature with small sample sizes. Future work with MRTA should focus on studies with the sample size exceeds the number of exploratory TA parameters, methods to improve standardization across analysis platforms and different scanners and institutions, and large prospective validation studies.

References

1. Varghese BA, Cen SY, Hwang DH, Duddalwa VA. Texture Analysis of Imaging: What Radiologists Need to Know. Am J Roentgenol 2019;212:520-528.
2. Lubner MG, Smith AD, Sandrasegaran K, Sahani DV, Pickhardt PJ. CT Texture Analysis: Definitions, Applications, Biologic Correlates, and Challenges. Radiographics 2017; 37:1483-1503.
3. Yang F, Dogan N, Stoyanova R, Ford JC. Evaluation of radiomic texture feature error due to MRI acquisition and reconstruction: a simulation study utilizing ground truth. Phys Med 2018;50:26–36.
4. Mayerhoefer ME, Szomolanyi P, Jirak D, Materka A, Trattnig S. Effects of MRI acquisition parameter variations and protocol heterogeneity on the results of texture analysis and pattern discrimination: an application-oriented study. Med Phys 2009;36:1236–1243.
5. Materka A, Strzelecki M. On the effect of image brightness and contrast nonuniformity on statistical texture parameters. Foundations of Computing and Decision Sciences 2015;40:163–185.
6. van Griethuysen JJM, Fedorov A, Parmar C, et al. Computational Radiomics System to Decode the Radiographic Phenotype. Cancer Research 2017;77:e104–e107.
7. Miles KA, Ganeshan B, Hayball MP. CT texture analysis using the filtration-histogram method: what do the measurements mean? Cancer Imaging 2013;13:400-406.

8. Gourtsoyianni S, Ljungqvist G, Khan A, Glynne-Jones R, Ganeshan B, Miles KA, Goh V. Reproducibility of MRI texture analysis in primary rectal cancer, In European Society of Radiology 2013, Vienna, Austria.

9. Gourtsoyianni S, Doumon G, Prezzi D, et al. Primary rectal cancer: repeatability of global and local-regional MR imaging texture features. Radiology 2017;284:552-560.

10. Eng DJ, Dezortava M, Taimer P, Hajek M. Texture analysis of human liver. J Magn Reson Imaging 2002;15:68-74.

11. Mahnoud-Ghoneim D, Amin A, Corr P. MRI based texture analysis: a potential technique to assess protectors against induced liver fibrosis in rats. Radiol Oncol 2009;43:30-40.

12. Yu H, Buch K, Li B, et al. Utility of texture analysis for quantifying hepatic fibrosis on proton density MRI. J Magn Reson Imaging 2015;42:1259-1265.

13. Bahl G, Cruite I, Wolfson T, et al. Noninvasive classification of hepatic fibrosis based on texture parameters from double contrast enhanced magnetic resonance images. J Magn Reson Imaging 2012;36:1154-1161.

14. Leonie P, Guillame G, Nguyen BN, Tang A. Liver fibrosis quantification by magnetic resonance imaging. Top Magn Reson Imaging 2017;26:229-241.

15. Yu H, Touret A-S, Li B, et al. Application of Texture Analysis on Parametric T1 & T2 maps for detection of Hepatic Fibrosis. J Magn Reson Imaging 2016;45:250-259.

16. Canella R, Borhani AA, Tublin M, et al. Diagnostic value of MR based texture analysis for the assessment of hepatic fibrosis in patients with non-alcoholic fatty liver disease (NAFLD). Abdom Radiol 2019;44:1816-1824.
17. House MJ, Bangma SJ, Thomas M, Gan EK, et al). Texture based classification of liver fibrosis using MRI. J Magn Reson Imaging 2015;41:322-328.
18. Wu Z, Matsiu O, Kitao A, et al. Hepatitis related chronic liver cirrhosis; feasibility of texture analysis of MR images for classification of fibrosis stage and necroinflammatory activity grade. PLoS One 2015;10:e0118297.
19. Yu H, Buch K, Li B, et al. Utility of texture analysis of quantifying hepatic fibrosis on proton density MRI. J Magn Reson Imaging 2015;42:1259-1265.
20. Barry B, Buch K, Soto JA, et al. Quantifying liver fibrosis through the application of texture analysis to diffusion weighted imaging. Magn Reson Imaging 2014;32:84-90.
21. Xu J, Wang X, Jin Z, et al. Value of texture analysis on Gadoxetic acid-enhanced MR for detecting liver fibrosis in a rat model. Chin Med Sci J 2019;34:24-32.
22. Kato H, Kanematsu M, Zhang X, et al. Computer-aided diagnosis of hepatic fibrosis: preliminary evaluation of MRI texture analysis using the finite difference method and artificial neural network. Am J Roentgenol 2007;189:117-122.
23. Zang X, Gao X, Liu BJ, et al. Effective staging of fibrosis by the selected texture features of liver: Which one is better, CT or MR imaging? Comput Med Imaging Graph 2015;46:227-236.
24. Ariff B, Lloyd CR, Khan S, et al. Imaging of liver cancer. World J of Gasteroenterol 2009;15:289-300.

25. Li Z, Mao Y, Huang W, et al. Texture based classification of different single lesions based on SPAIR T2W MRI images. BMC Med Imaging 2017;17:42.

26. Nault JC, Couchy G, Balaband G, et al. Molecular classification of hepatic adenoma associates with risk factors, bleeding and malignant transformation. Gasteroenterology 2017;152:880-894.

27. Guo Y, Li W, Zhang Y, et al. Diagnostic value of Gadoxetic acid-enhanced MR imaging to distinguish HCA and its subtype from FNH: a systematic review. Int J Med Sci. 2017;14:668-674.

28. Canella R, Rangaswamy B. Minervini MI, et al. Value of texture analysis on Gadoxetic acid enhanced MRI for differentiating hepatocellular adenoma from focal nodular hyperplasia. Am J Roentgenol 2019;21:538-546.

29. Stocker D, Marquez HP, Wagner MW, et al. MRI texture analysis for differentiation of malignant and benign hepatocellular tumors in the non-cirrhotic liver. Heliyon 2018;4:e00987.

30. Parkin DM, Bray F, Ferlay J, et al. Estimating the world cancer burden: Int J Cancer 2001;94:153-156.

31. Bruix J, Sherman M. Management of hepatocellular carcinoma. Hepatology 2005;42:1208-1236.

32. Zhou W, Zhang L, Wang K, et al. Malignancy characterization of hepatocellular carcinomas based on texture analysis of contrast-enhanced MR images. J Magn Reson Imaging 2017;45:1476-1484.

33. Roayie S, Obeidat K, Sposito C, et al. Resection of hepatocellular cancer <2 cm: results from 2 western centers. Hepatology 2013;57:1426-1435.

34. Shah SA, Cleary SP, Wei AC, et al. Recurrence after liver resection for hepatocellular carcinoma: risk factors, treatment, outcomes. Surgery 2007;141:330-339.

35. Choi GH, Kim DH, Kang Cm, et al. Prognostic factors and optimal treatment strategy for intrahepatic nodular recurrence after curative resection of hepatocellular carcinoma. Ann Surg Oncol 2008;15:618-629.

36. Ahn SJ, Kim JH, Park SJ, et al. Hepatocellular carcinoma: preoperative Gadoxetic acid-enhanced MR imaging can predict early recurrence after curative resection using image features and texture analysis. Abdom Radiol 2019;44:539-548.

37. Hui TCH, Chuah TK, Low HM, et al. Predicting early recurrence of hepatocellular carcinoma with texture analysis of preoperative MRI. A radiomics study. Clin Radiology 2018;73:1056.e11-1056.e16.

38. Yu JY, Zhang HP, Tang ZY, et al. Value of texture analysis based on enhanced MRI for predicting an early therapeutic response to trans-catheter arterial chemoembolization combined with high-intensity focused ultrasound treatment in hepatocellular carcinoma. Clin Radiology 2018;73:758.e9-758.e18.

39. Reimer RP, Reimer P, Mahnken AH. Assessment of therapy response to transarterial radioembolization for liver metastases by means of post-treatment MRI-based texture analysis. Cardiovasc Intervent Radiol 2018;41:1545-1556.

40. Zhang H, Li W, HU F, et al. MR texture analysis: potential imaging biomarker for predicting the chemotherapeutic response of patients with colorectal liver metastasis. Abdom Radiol 2019;44:65-71.
41. Delongchampes NB, Rouanne M, Flam T, et al. Multiparametric magnetic resonance for the detection and localization of prostate cancer: combination of T2-weighted, dynamic contrast enhanced and diffusion weighted imaging. BJU Int 2011;107:1411-1811.
42. Wibmer A, Hricak H, Gondo T, et al. Harlick texture analysis of prostate MRI: utility for differentiating non-cancerous prostate from prostate cancer and differentiating prostate cancers with different Gleason Scores. Eur Radiol 2015;25:2840-2850.
43. Hameed M, Ganeshan B, Shur J, et al. The clinical utility of prostate cancer heterogeneity using texture analysis of multi-parametric MRI. Int Urol Nephrol 2019;51:817-824.
44. Nketiah G, Elschot M, Kim E, et al. T2-weighted MRI derived textural features reflect prostate cancer aggressiveness: preliminary results. Eur Radiol 2017;27:3050-3059.
45. Rozenberg R, Thornhill RE, Flood TA, et al. Whole-tumor quantitative apparent diffusion coefficient histogram and texture analysis to predict Gleason score upgrading in intermediate – risk 3+4=7 Prostate Cancer. Am J Roentgenol 2016;206:775-782.
46. Langer DL, van der Kwast TH, Evans AJ, et al. Prostate Cancer detection with multi-parametric MRi : logistic regression analysis of quantitative T2, diffusion-weighted imaging and dynamic contrast enhanced MRI. J Magn Reson Imaging 2009;30:327-334.

47. Sidhu HS, Benigno S, Ganeshan B, et al. Texture analysis of multi-parametric MRI detects transition zone prostate cancer. Eur Radiol 2017;27:2348-2358.

48. Orcyz C, Villers A, Rusinek H, et al. Prostate cancer heterogeneity: texture analysis score based on multiple magnetic resonance imaging sequences for detection, stratification and selection of lesions at time of biopsy. BJU Int 2019;124:76-86.

49. Duda D, Kretowski M, Matheiu R, et al. Multi-sequence texture analysis in classification of in vivo MR images of the prostate. Biocybernetics and Biomedical Engineering 2016;36:537-552.

50. Rais-Bahrami S, Siddiqui M, Vourganti S, et al. Diagnostic value of bi-parametric magnetic resonance imaging (MRI) as an adjunct to prostate specific antigen (PSA) – based detection of prostate cancer in men without prior biopsies. BJU Int 2015;115:381-388.

51. Stanzione A, Imbriaco M, Cocozza S, et al. Biparametric 3T magnetic resonance imaging for prostate cancer detection in biopsy naïve patient population: a further improvement of PIRADS v2? Eur J Radiol 2016;18:2269-2274.

52. Niu X, Chen Z, Chen L, et al. Clinical application of bi-parametric MRI texture analysis for detection and evaluation of high grade prostate cancer in zone specific regions. AJR 2018;210:549-556.

53. D'Amico AV, Whittington R, Malkowwicz S, et al. Biochemical outcome after radical prostatectomy, external beam radiation therapy, or interstitial radiation therapy for clinically localized prostate cancer. JAMA 1998;280:969-974.

54. Gnep K, Fargeas A, Guitierrez-Carvajal RE, et al. Haralick textural features on T2-weighted MRI are associated with biochemical recurrence following radiotherapy for peripheral zone prostate cancer. J Magn Reson Imaging 2017;45:103-117.

55. Han M, Partin AW. Nomograms for clinically localized prostate cancer. Part I: radical prostatectomy. Semin Urol Oncol 2002;20:123-130.

56. Kattan MW, Eastham JA, Stapleton AM et al. A preoperative nomogram for disease recurrence following radical prostatectomy for prostate cancer. J Natl Cancer Inst 1998;90:766-771.

57. Poulakis V, Witzsch U, De Vries R, et al. Pre-operative neural network using combined magnetic resonance imaging variables, Prostate Specific Antigen and Gleason score for predicting prostate cancer biochemical recurrence after radical prostatectomy. Urology 2004;64:1165-1170.

58. Carlin BI, Andriole GI. The natural history, skeletal complications and management of bone metastasis in patients with prostate carcinomas. Cancer 2000;88:2989-2994.

59. Jambor I, Kuisma A, Ramadan S, et al. Prospective evaluation of planar bone scintigraphy , SPECT, SPEC/CT, 18F-NaF PET/CT and whole body 1.5T MRI, including DWI, for the detection of bone metastasis in high risk breast and prostate cancer patients. SKELETA Clinical Trial, Acta Oncol 2016;55:59-67.

60. Perez-Lopez R, Mateo J, Mossop H, et al. Diffusion weighted imaging as a biomarker for evaluating metastasis on prostate cancer: a pilot study: Radiology 2017;28:168-177.

61. Reischauer C, Patzwahl R, Koh DM, et al. Texture analysis of apparent diffusion coefficient maps for treatment response assessment in prostate cancer metastases - A pilot study. Eur J Radiol 2018;101:184-190.

62. Hotker Am, Garcia-Aguilar J, Gollub MJ. Multiparametric MRI of rectal cancer in the assessment of response to therapy: a systematic review. Dis Colon Rectum 2014;57:790-798.

63. Blazic IM, Campbel NM, Gollub MJ. MRI for evaluation of treatment response in rectal cancer. Br J Radiol 2016;89:20150964.

64. Beets-Tan RG, Beets GL, Vliegen RF, et al. Accuracy of magnetic resonance imaging in prediction of tumor free restriction margin in rectal cancer surgery. Lancet 2001;357:497-504.

65. Nagtegaal ID, Quirke P. What is the role for the circumferential margin in the modern treatment of rectal cancer? J Clin Oncol 2008;26:303-312.

66. Beets-Tan RG, Beets GL. Local staging of rectal carcinoma: review of imaging. J Magn Reson Imaging 2011;33:1012-1019.

67. De Cecco CN, Ganeshan B, Ciolina M, et al. Texture analysis as imaging biomarker of tumoral response to neoadjuvant chemotherapy in rectal cancer patients studied with 3T magnetic resonance. Invest Radiol 2015;4:239-245.

68. O'Conner JP, Rose CJ, Jackson A, et al. DCE-MRI biomarkers of tumor heterogeneity predict CRC liver metastasis shrinkage following bevacizumab and FOLFOX-6. Br J Cancer 2001;105:139-145.

69. Alic L, Vliet M, van Dijke CF, Eggrmont AM, et al. Heterogeneity in DCE-MRI parametric maps: a biomarker for treatment response? Phys Med Biol 2011;56:1601-1616.

70. Van der Paardt MP, Zagers MB,Beets-Tan RG, et al. Patients who undergo pre-operative chemoradiotheray for locally advanced rectal cancer restaged by using diagnostic MRI imaging: a systemic review and meta-analysis. Radiology 2013;269:101-112.

71. Yang L, Qiu M, Xia C, et al. Value of high resolution DWI in combination with texture analysis for the evaluation of tumor response after pre-operative chemoradiotherapy for locally advanced rectal cancer. Am J Roentgenol 2019;212:1-8.

72. Aker M, Ganeshan B, Afaq A, et al. Magnetic resonance texture analysis in identifiying complete pathological response to neoadjuvant treastment in locally advanced rectal cancer. Dis Colon Rectum 2019;62:163-170.

73. Nardone V, Reginelli A, Scala F, et al. Magnetic Resonance Imaging texture analysis predicts early progression in rectal cancer patients undergoing neoadjuvant chemoradiation. Gastroenterol Res Pract 2019;2019:8505798.

74. Jalil O, et al. Magnetic resonance based texture parameters as potential imaging biomarkers for predicting long-term survival in locally advanced rectal cancer treated by chemoradiotherapy. Colorectal Dis 2017;19:349-362. (ref #71)

75. Shuch B, Amin A, Armstrong AJ, et al. Understanding pathological variants of renal cell carcinoma: distilling therapeutic opportunities from biologic complexity. Eur Urol 2015;67:85-97.

76. Singer E, Bratslavsky G, Linehan W, et al. Targeted therapies for non-clear renal cell carcinoma . Target Oncol 2010;5:119-129.

77. Hallscheidt PJ, Bock M, Reidasch G, et al. Diagnostic accuracy of staging renal cell carcinomas using multidetector-row computed tomography and magnetic resonance imaging : a prospective study with histopathological correlation. J Comput Assist Tomogr 2004;28:333-339.

78. Kierans AS, Rusinek H, Lee A, et al. Textural differences in apparent diffusion coefficient between low and high stage clear cell renal cell carcinoma. AJR 2014;203:W637-W644.

79. Pignot G, Elie C, Conquy S, et al. Survival analysis of 130 patients with papillary renal cell carcinoma: prognostic utility of type 1 and type 2 sub-classification. Urology 2007;69:230-235.

80. Doshi AM, Ream JM, Kierans AS, et al. Use of MRI differentiation of papillary renal cell carcinoma subtypes: Qualitative and quantitative analysis. Am J Roentgenol 2016;206:566-572.

81. Vendrami CL, Velichko YS, Miller FH, et al. Differentiation of papillary renal cell carcinoma subtypes on MRI: Qualitative texture analysis. Am J Roentgenol 2018;211:1234-1245.

82. Goyal A, Razik A, Kandasamy D, et al. Role of MR texture analysis in histological subtyping and grading of renal cell carcinoma: a preliminary study. Abdom Radol (NY) 2019;44:3336-3349.

83. Conlon KC, Klimstra DS, Brennan MF. Long-term survival after curative resection for pancreatic ductal adenocarcinoma. Clinico-pathologic analysis of 5-year survivors. Ann Surg 1996;223:273-279.

84. Treadwell JR, Zafar HM, Mitchell MD, et al. Imaging tests for the diagnosis and staging of pancreatic adenocarcinoma: a meta-analysis. Pancreas 2016;45:789-795.

85. Cassinoto C, Chong J, Zougopoulos G, et al. Resectable pancreatic adenocarcinoma: role of CT quantitative imaging biomarkers for predicting pathology and patient outcomes. Eur J Radiol 2017;90:152-158.

86. Eilaghi A, Baig S, Zhang Y, et al. CT texture features are associated with overall survival in pancreatic ductal adenocarcinoma – a quantitative analysis. BMC Med Imaging 2017;17:38.

87. Choi MH, Lee YJ, Yoon SB, et al. MRI of pancreatic ductal adenocarcinoma: texture analysis of T2-weighted images for predicting long-term outcome. Abdom Radiol 2019;44:122-130.

88. Amant F, Moerman P, Neven P, et al. Endometrial Cancer. Lancet 2005;366:491-505.

89. Creutzberg CL, van Putten WL, Koper PC, et al. Surgery and post-operative radiotherapy versus surgery alone for patients with stage 1 endometrial cancer: multicenter randomized trial. PORTEC study group. Post-operative radiation therapy in Endometrial Cancer. Lancet 2000;355:1404-1411.

90. Keys HM, Roberts JA, Brunetto VL, et al. A phase III trial of surgery with or without adjunctive external pelvic radiation therapy in intermediate risk endometrial

adenocarcinoma: A gynecologic Oncology Study Group. Gynecol Oncol 2004;94:241-242.

91. Gadduci A, Cavazzana A, Cosio S, et al. Lymph-vascular space involvement and outer third myometrial invasion are strong predictors of distant hematogenous failures in patients with stage I-II endometroid type endometrial cancer. Anticancer Res 2009;29:1715-1720.

92. Hricak H, Rubinstein L, Gherman G, et al. MR imaging evaluation of endometrial carcinoma: results of an NCI cooperative study. Radiology 1991;17:829-832.

93. Sironi S, Colombo E, Villa G, et al. Myometrial invasion by endometrial carcinoma: assessment with plain and gadolinium-enhanced MR imaging. Radiology 1992;185:207-212.

94. Savci G, Ozyaman T, Tutar M, et al. Assessment of depth of myometrial invasion by endometrial cancer: comparison of T2-weighted SE and contrast enhanced dynamic GRE MR imaging. Eur Radiol 1998;8:218-223.

95. Das SK, Niu XK, Wang JL, et al. Usefulness of DWI in preoperative assessment of deep myometrial invasion in patients with endometrial carcinoma: a systematic review and meta-analysis. Cancer Imaging 2014;14:32.

96. Ueno Y, Forghani B, Forghani R, et al. Endometrial Carcinoma: MR imaging based texture model for pre-operative risk stratification-A preliminary analysis. Radiology 2017;284:748-757.

97. Ytre-Hauge S, et al. Preoperative tumor texture analysis on MRI predicts high-risk disease and reduced survival in endometrial cancer. J Magn Reson Imaging 2018;48:1637-1647.

98. Harrison L, Dastidar P, Eskola H, et al. Texture analysis on MRI images of non-Hodgkin lymphoma. Comput Biol Med 2008;38:519-524.

99. Makanyanga J, Ganeshan B, Rodriguez-Justo M, et al. MRI texture analysis (MRTA) of T2-weighted images in Crohn's disease may provide information on histological and MRI disease activity in patients undergoing ileal resection. Eur Radiol 2017;27:589-597.

100. Bhatnagar G, Makanyanga J, Ganeshan B, et al. MRI texture analysis parameters of contrast-enhanced T1-weighted images of Crohn's disease differ according to the presence or absence of histological markers of hypoxia and angiogenesis. Abdom Radiol (NY) 2016;41:1261-1269.

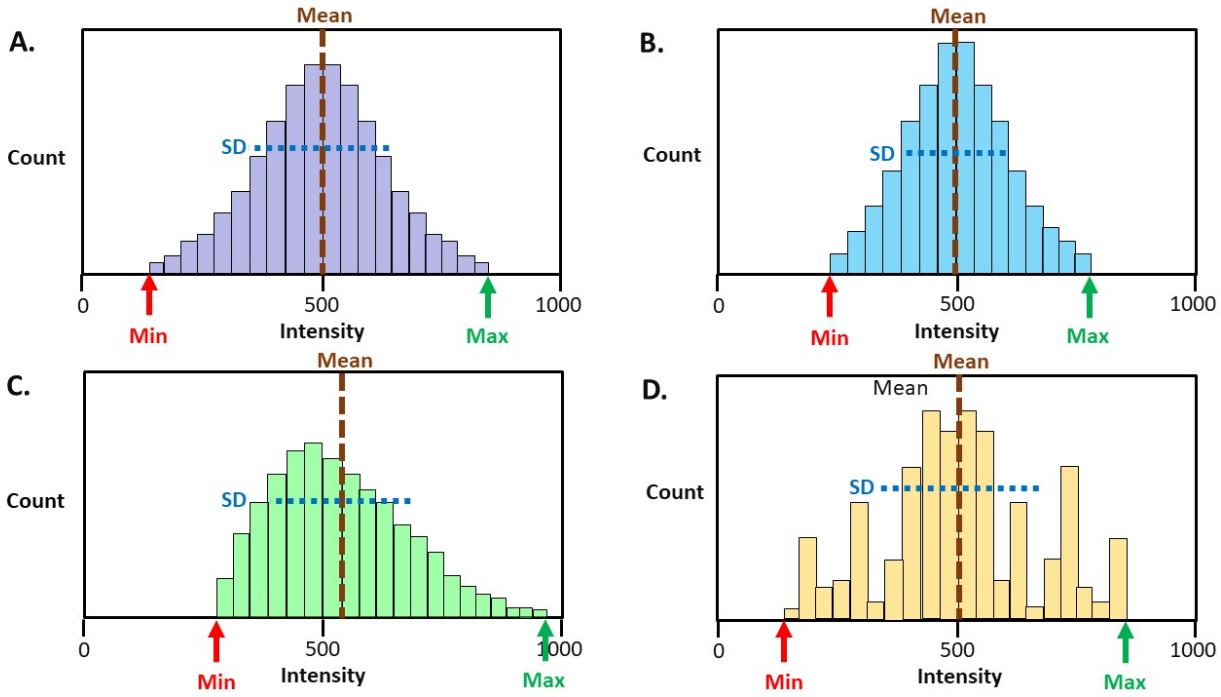

Figure 1. Histograms illustrating common first order texture analysis parameters. Histograms A. and B. have normal distributions and identical means, but B. has a smaller standard deviation (SD), smaller range, and higher kurtosis. Histograms C. and A. have identical range, but C. has a rightward skew and slightly higher mean and SD. Histograms D. and A. have identical mean and range, but histogram D. has high entropy and a higher SD. Notice that the evaluation of multiple parameters better describes the shape of the histograms and also better differentiates the histograms from one another.

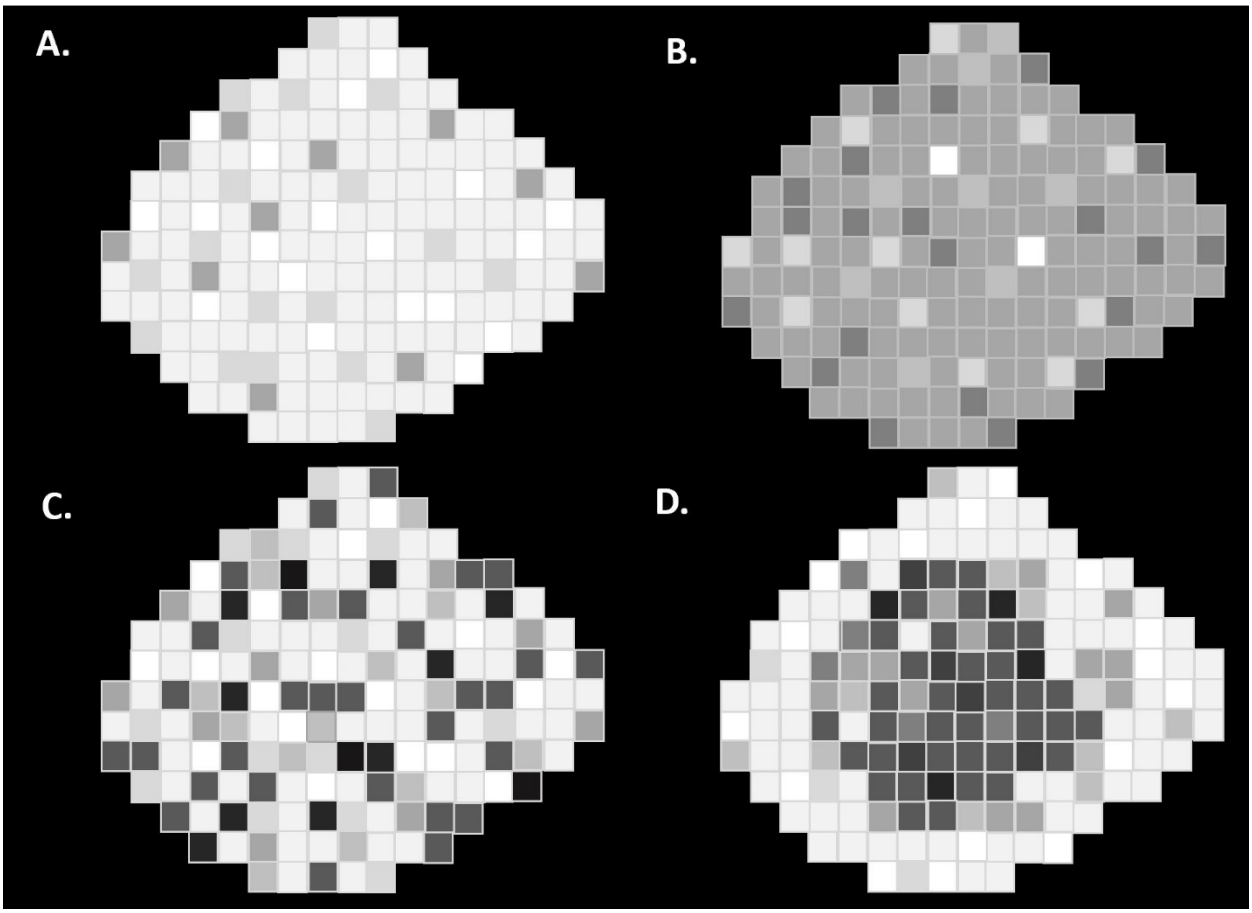

Figure 2. Simulated renal masses are depicted after segmentation on contrast-enhanced fat-saturated T1W images. The renal mass in A. has homogeneous hyperenhancement which would correspond to a high mean and low standard deviation (SD) and entropy. The renal mass in B. has homogenous hypoenhancement which would have low mean, SD, and entropy, with the low mean differentiating it from the renal mass in A. The renal mass in C. is diffusely heterogeneous, which would correspond to an intermediate mean, high SD and changes in kurtosis, skewness, and entropy compared to the renal masses in A. or B. The renal mass in D. is also heterogeneous but has peripheral hyperenhancement and central hypoenhancement due to central necrosis. This mass would also have an intermediate mean, high SD and changes in

kurtosis and skewness as well as changes in one or more second order statistical methods when compared to the renal masses A, B, or C.

Note - Definition of commonly used first-order statistics including mean (average brightness), standard deviation (width of the histogram or deviation from average), threshold (percentage of pixels within a specified range of intensities), minimum (lowest intensity value), maximum (highest intensity value), skewness (asymmetry in the frequency of pixel intensities), kurtosis (pointiness of the pixel histogram), and entropy (irregularity of the pixel intensities)

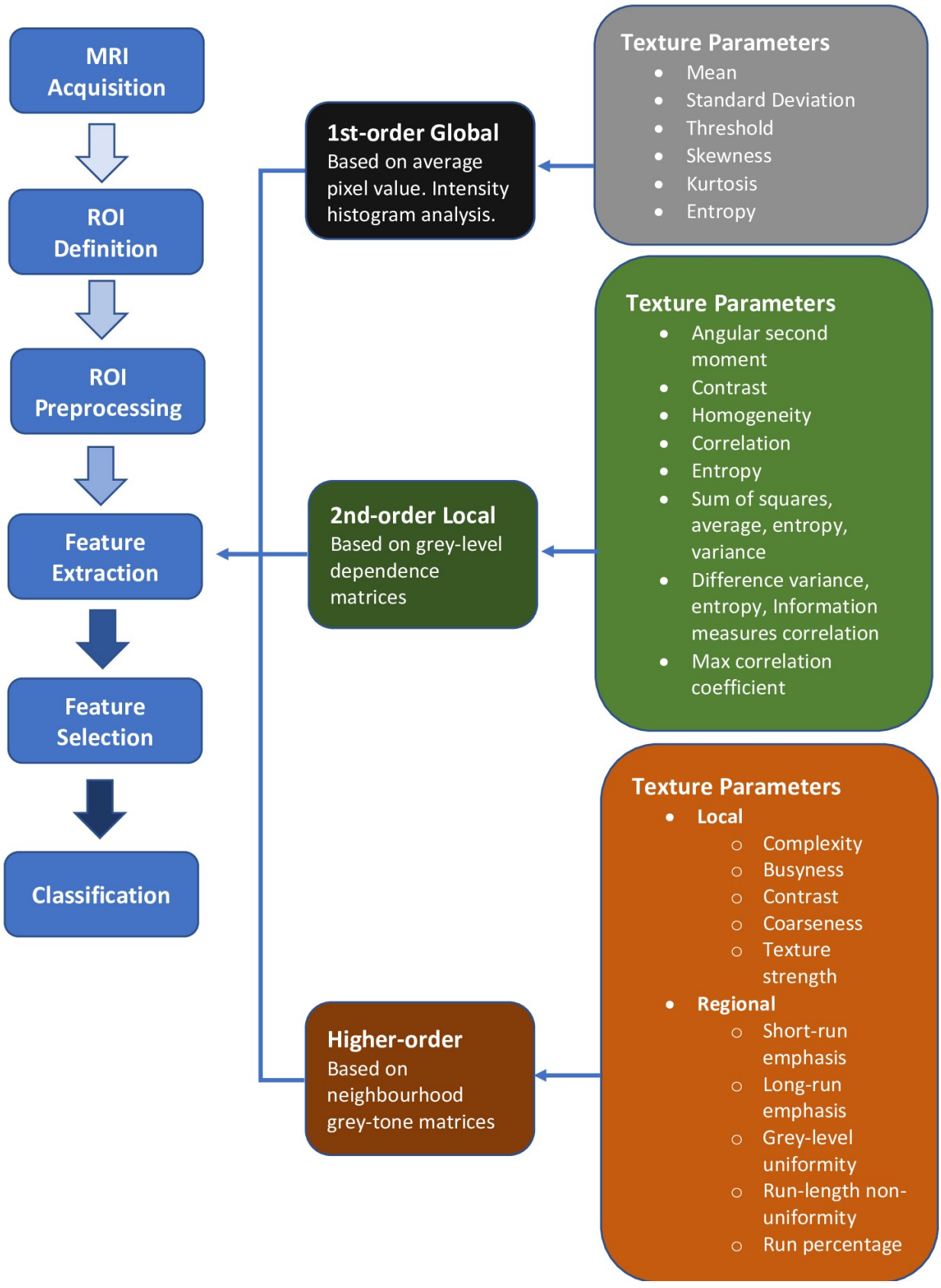
MRI Acquisition
ROI Definition
ROI Preprocessing
Feature Extraction
Feature Selection
Classification
1st-order Global
Based on average pixel value. Intensity histogram analysis.
2nd-order Local
Based on grey-level dependence matrices
Higher-order
Based on neighbourhood grey-tone matrices
Texture Parameters
Mean
Standard Deviation
Threshold
Skewness
Kurtosis
Entropy
Texture Parameters
Angular second moment
Contrast
Homogeneity
Correlation
Entropy
Sum of squares, average, entropy, variance
Difference variance, entropy, Information measures correlation
Max correlation coefficient
Texture Parameters
Local
Complexity
Busyness
Contrast
Coarseness
Texture strength
Regional
Short-run emphasis
Long-run emphasis
Grey-level uniformity
Run-length non-uniformity
Run percentage

Figure 3. A flowchart depicts the steps involved in MRI texture analysis. Feature extraction can be performed with a wide variety of texture parameters, with examples depicted and categorized by statistical order.

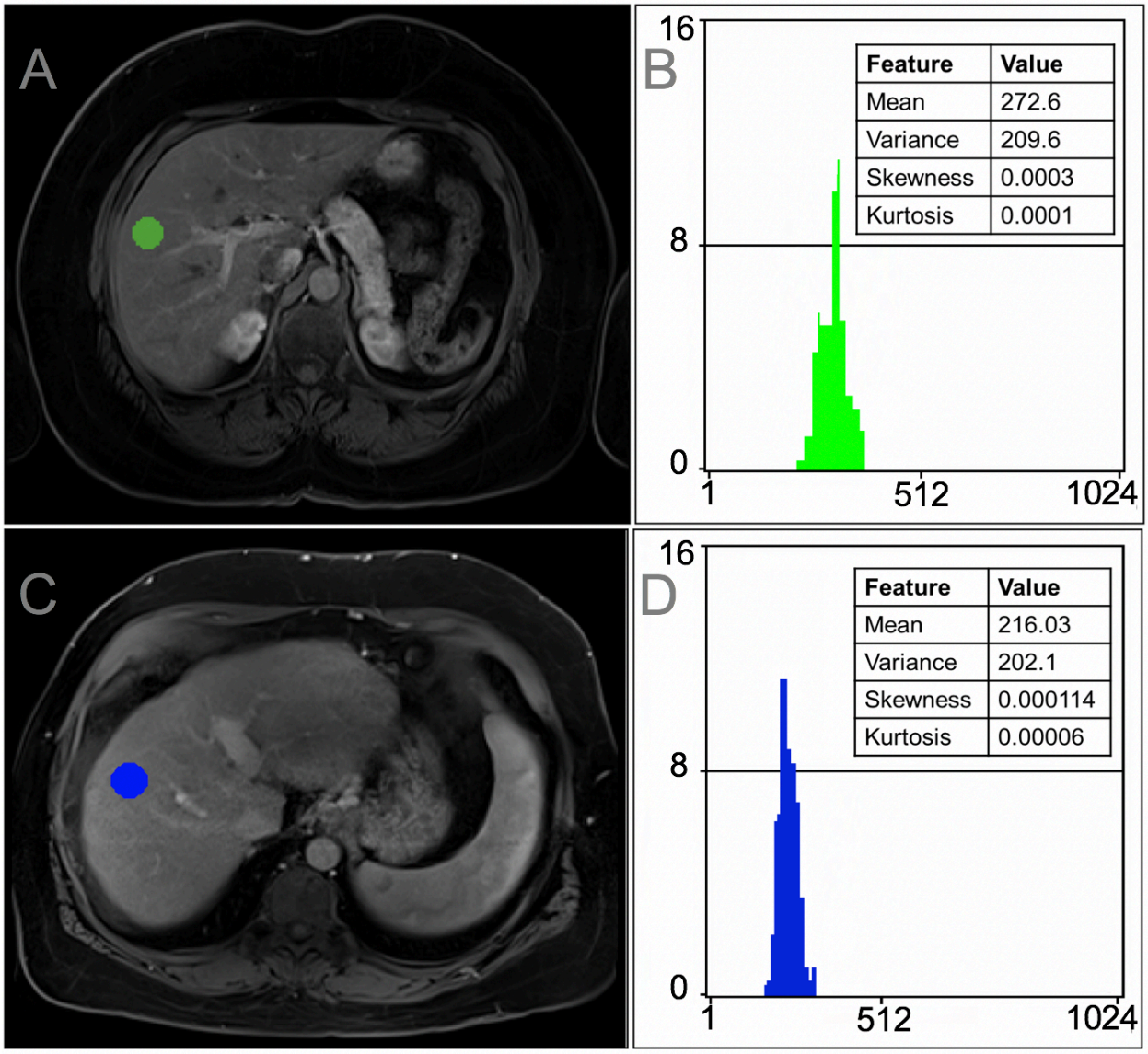

Figure 4. 56-year-old healthy male with a normal liver on post-contrast T1-weighted fat-saturated images with a region of interest (A, green) and corresponding histogram (B) with relatively high mean intensity values. 54-year-old male with cirrhotic liver on post-contrast T1-weighted fat-saturated images with a region of interest (C, blue) and corresponding histogram (D) with relatively low mean intensity values. Other texture parameters for each are also shown to the right of the histograms.

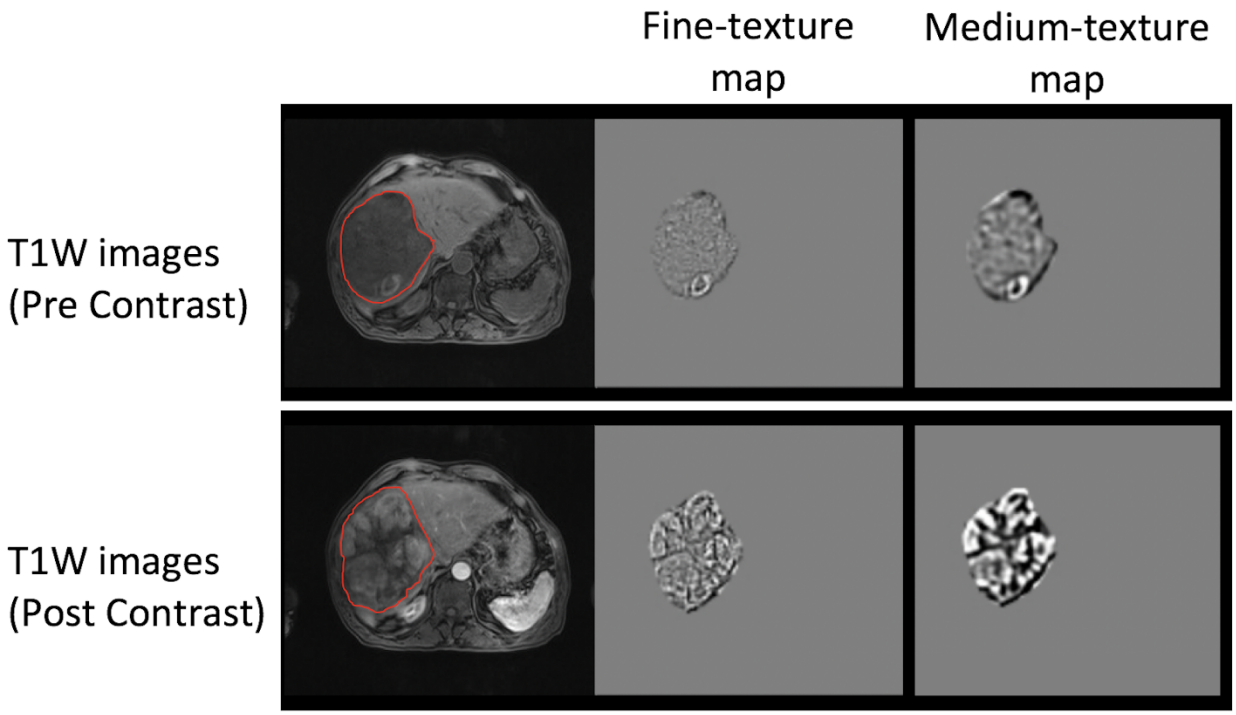

Figure 5. 61-year-old male with cirrhosis and regions of interest around the large hepatocellular carcinoma (red) on pre- and post-contrast T1-weighted fat-saturated images. The regions of interest have been processed with Laplacian of Gaussian image filters to depict fine-texture and medium-texture maps. This technique highlights different texture features that are visible in the post-processed images and that can be quantified subsequently by MRI texture analysis.

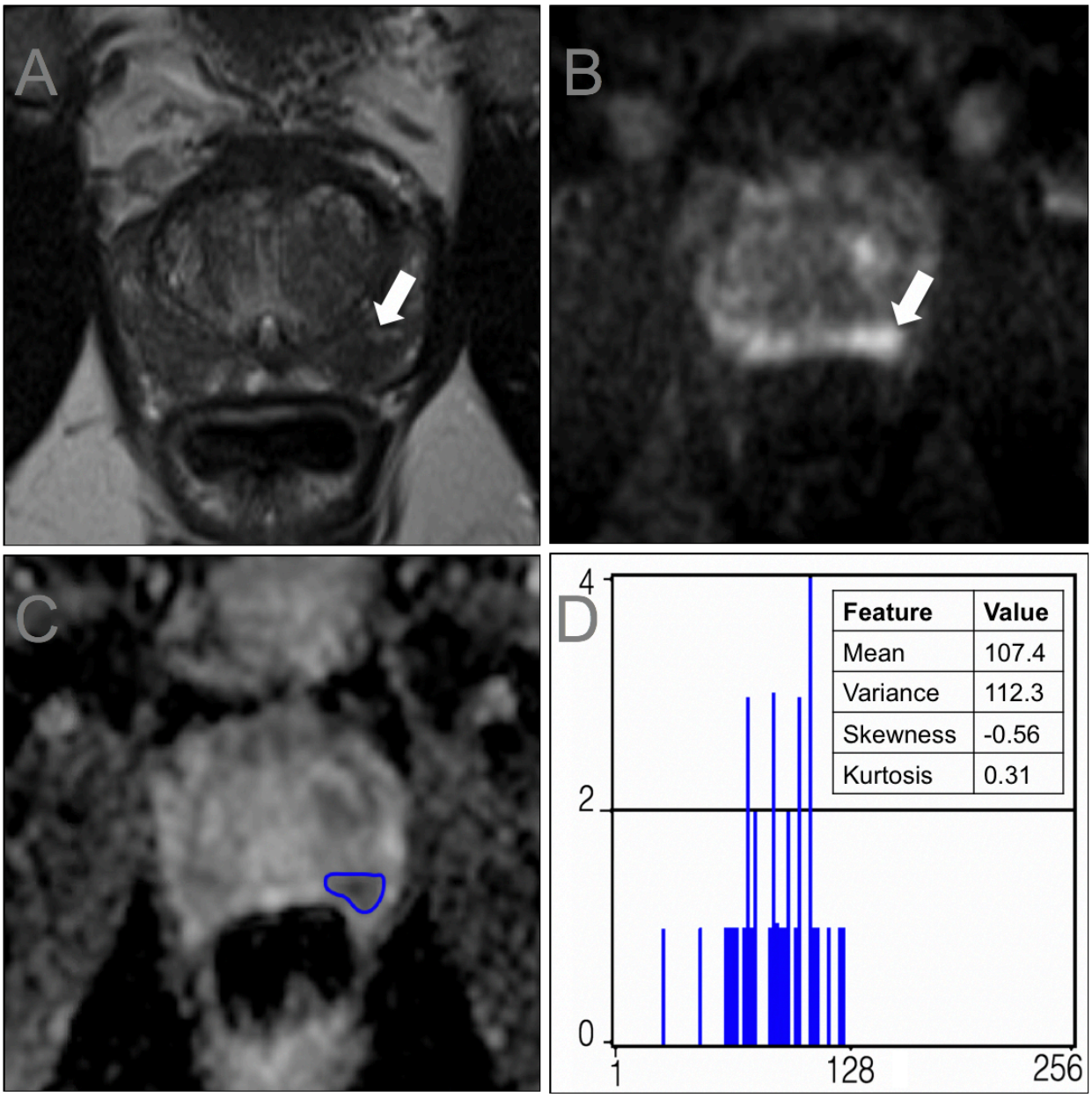

Figure 6. 64-year-old male with elevated PSA (4.9 ng/mL). A prostate MRI was performed, and the T2-weighted image shows a lesion in left peripheral zone with low signal T2W images (A), high signal on high B-value diffusion weighted images (B), low signal on apparent diffusions coefficient images (C). The lesion is segmented in apparent diffusion weighted images (C), and the corresponding histogram is shown (D). On subsequent ultrasound-guided biopsy, the lesion was a Gleason score 3+5=8 adenocarcinoma.